Chinese Journal of Catalysis 34 (2013) 1697–1704

available at www.sciencedirect.com

ScienceDirect

journal homepage: www.elsevier.com/locate/chnjc

Article

$CoFe_2O_4$ nanoparticles: An efficient heterogeneous magnetically separable catalyst for "click" synthesis of arylidene barbituric acid derivatives at room temperature

Jaspreet Kaur Rajput *, Gagandeep Kaur

Department of Chemistry, Dr. B. R. Ambedkar National Institute of Technology, Jalandhar-144011, India

ARTICLE INFO

Article history:
Received 9 May 2013
Accepted 5 June 2013
Published 20 September 2013

Keywords:
Magnetically separable catalyst
Arylidene barbituric acid derivative
Aqueous ethanol
Superparamagnetic $CoFe_2O_4$ nanoparticle
Heterogeneous catalyst

ABSTRACT

A coprecipitation method was used to synthesize superparamagnetic $CoFe_2O_4$ nanoparticles without using any capping agents/surfactants. The prepared nanoparticles were characterized using Fourier transform infrared spectroscopy, scanning electron microscopy, transmission electron microscopy, X-ray diffraction, a vibrating sample magnetometer (VSM), N_2 adsorption and thermogravimetric/differential thermal analysis/differential thermal gravimetry techniques. The synthesized spinel $CoFe_2O_4$ nanoparticles had an average size of 2–8 nm with a high surface area (140.9 m^2/g). The field-dependent magnetization, demonstrated by VSM and saturation magnetization, was found to be 1.77 emu/g. An efficient method was used for the synthesis of arylidene barbituric acid derivatives using $CoFe_2O_4$ magnetic nanoparticles as a magnetically separable and reusable catalyst in aqueous ethanol. The attractive features of this synthetic protocol were very short reaction time, high yields, high turnover frequency, simple work-up procedure, economy, a clean reaction methodology, and chemoselectivity, as well as provision of an ecofriendly and green synthesis.

1. Introduction

The main goal in the field of catalysis, in terms of green chemistry, is to develop environmentally benign, practical, clean, economical, and efficient processes for catalyst separation and recycling [1]. A possible way of achieving this is the use of magnetic catalyst systems for various organic transformations. A magnetic catalyst system provides more effective separation of the catalyst than do traditional filtration and centrifugation methods as it avoids catalyst loss [2]. Furthermore, magnetic separation is economical, simple, and promising for industrial application [3–5]. In recent years, magnetic nanoparticles have attracted worldwide attention as efficient, economical, environmentally friendly, and recyclable catalysts [6–14]. Magnetic nanoparticles are also used as alternatives to conventional heterogeneous supports. In this context, magnetic ferrite nanoparticles such as cobalt ferrite nanoparticles have been used as magnetically separable catalysts because they have high thermal stability, large magnetic anisotropies, high surface areas, moderate saturation magnetizations, and chemical stability [15,16]; their catalytic properties depend on the tetrahedral and octahedral sites of the spinel structure of ferrite nanoparticles. Various methods have been reported for the synthesis of cobalt ferrite nanoparticles, such as sonochemical [17], microemulsion [18], mechanochemical [19], and coprecipitation [20–22] methods. The most commonly used and effective method is coprecipitation, as low-temperature coprecipitation provides homogeneous and finely powdered ferrite nanoparticles with high surface areas and better catalytic activity [23].

* Corresponding author. Tel: +91-181-2690301-02 PBX Extn: 2208; Fax: +91-181-2690320; E-mail: rajputj@nitj.ac.in
DOI: 10.1016/S1872-2067(12)60646-9 | http://www.sciencedirect.com/science/journal/18722067 | Chin. J. Catal., Vol. 34, No. 9, September 2013

In this study, we developed a magnetically separable nanocatalyst that is simple to produce, green, efficient, and inexpensive and exhibits excellent catalytic performance in the synthesis of arylidene barbituric acid derivatives. The catalyst was easily separated from the reaction mixture using an external magnet and was reusable without significant loss of catalytic activity.

Barbituric acid derivatives are of great interest because of their diverse biological activity, e.g., antibacterial, hypotensive, anesthetic, antitumor, and sedative effects [24–26]; they are also used as intermediates in the synthesis of benzyl barbituric derivatives [27], heterocyclic compounds [28], and oxadeazaflavines [29]. In addition to these kinds of application, some of these derivatives have been investigated as non-linear optical materials [30] and dyes [31].

The synthesis of arylidene barbituric acids has been carried out by condensation of aromatic aldehydes with barbituric acid. Various reagents/methods have been reported in the literature, e.g., basic alumina [32], infrared (IR) irradiation [33], microwave irradiation [34], NH_2SO_3H [35], Ni nanoparticles [36], L-proline [37], $BiCl_3$ [38], $Ce_1Mg_xZr_{1-x}O_2$ [39], ionic liquids [40], $SiO_2{\cdot}12WO_3{\cdot}24H_2O$ [41], and triethylbenzyl ammonium chloride (TEBA) [42]. However, most of the protocols/reagents suffer from shortcomings such as lengthy reaction time, expensive/toxic/unavailable reagents, high-temperature conditions, hazardous solvents, formation of undesirable products, low yields, non-recyclability, and difficult catalyst separation. To overcome these drawbacks, and in continuation of our previous work on green catalysis [43] and nanomaterials [44,45], we used cobalt ferrite as a heterogeneous catalytic system.

In this paper, we highlight our work on the synthesis of magnetically recoverable superparamagnetic cobalt ferrite magnetic nanoparticles of high surface area as a catalyst, and a simple, efficient, green protocol for the synthesis of arylidene barbituric acid derivatives.

2. Experimental

2.1. Preparation of cobalt ferrite nanoparticles

The cobalt ferrite nanoparticles were synthesized using the chemical coprecipitation technique [46], with minor modifications. The $CoFe_2O_4$ nanoparticles were prepared by coprecipitation of $FeCl_3$ and $CoCl_2{\cdot}6H_2O$ in a basic solution under ultrasonication. $FeCl_3$ (9.3 mmol) and $CoCl_2{\cdot}6H_2O$ (4.2 mmol) were separately dissolved in deionized water (50 ml) and placed in an ultrasonicator. An aqueous solution of KOH (3 mol/L, 25 ml) was added under ultrasonication and the mixture was sonicated for 30 min. A black dispersion was formed during sonication, and the black precipitate was separated out using an external magnet, washed with large amounts of Millipore water, and then washed with ethanol. The product was then dried in an oven at 100 °C for 1 h and stored for further use.

2.2. Characterization of cobalt ferrite nanoparticles

The crystal structure of the cobalt ferrite nanoparticles was determined by X-ray diffraction (XRD) using a Panlytical XPERTPRO (NPD) X-ray diffractometer with Cu K_α radiation (λ = 0.154 nm), in the 2θ range 20°–80°. Fourier transform IR (FT-IR) spectroscopy was carried out in the range 400–4000 cm^{-1} with a Perkin Elmer Spectrum RX-IFTIR, using KBr pellets. The formation of $CoFe_2O_4$ nanoparticles was confirmed by scanning electron microscopy/energy-dispersive X-ray spectroscopy (SEM-EDX) analysis, which was carried out using a JEOL JSM-6610LV. The $CoFe_2O_4$ morphology was studied using transmission electron microscopy (TEM). The sample was prepared by ethanol dispersion of nanoparticles, which were deposited on a carbon-coated Cu grid, and after drying, analysis was performed using a Hitachi S7500 instrument. The magnetic properties were measured using a vibrating sample magnetometer (VSM, Princeton Applied Research model 155) at room temperature with a maximum magnetic field range of +1 T to −1 T.

Thermogravimetric analysis (TGA), differential thermal analysis (DTA), and differential thermal gravimetry (DTG) were performed on the catalyst using an EXSTAR6000 TG/DTA 6300 instrument in the temperature range 50–700 °C at a heating rate of 10 °C/min in a Pt an under an air atmosphere. The specific surface area of the catalyst was determined using a Quantachrome NOVA-4000e instrument at liquid-nitrogen temperature with vacuum degassing at 110 °C for 3 h. The specific surface area was obtained using the BET equation.

2.3. Synthesis of arylidene barbituric acid derivatives

All reactions were carried out using reagent-grade solvents and the reagents were purchased from a local supplier. An ELIX 3 Millipore apparatus was used to provide deionized water. Ultrasonication was carried out using a Loba Chemie 3.5L100H1DTC ultrasonicator.

Barbituric acid (5 mmol) was dissolved in a water-ethanol mixture (1:1, 5 ml), followed by addition of an aromatic aldehyde (5 mmol). The $CoFe_2O_4$ nanoparticle catalyst (5 mol% or 0.0117 g) was added to the reaction mixture and the mixture was stirred until completion of the reaction. After the reaction was complete, the catalyst was separated using a magnetic separator, washed with ethanol, and then dried at 70 °C for 1 h. The solid crude product was washed with water and dried. The product was further purified by recrystallization from ethanol. The synthesized arylidene barbituric acid derivatives were characterized using FT-IR and ^{1}H nuclear magnetic resonance (NMR) spectroscopies. Melting points were recorded using a Gallenkamp instrument and are uncorrected. ^{1}H-NMR (400 MHz) spectra were obtained with a Brucker Advance 400 spectrometer ($CDCl_3$) using tetramethylsilane as the internal standard. The entry numbers refer to Table 2.

3a. m.p. 262–264 °C. FT-IR (KBr, cm^{-1}): 3210, 3059, 1750, 1670. ^{1}H-NMR (400 Hz DMSO-d_6, δ): 7.42–8.11 (m, 5H), 8.37 (s, 1H), 11.28 (s, 1H, NH), 11.42 (s, 1H, NH). ^{13}C-NMR: 163.9, 162.2, 155.7, 151, 133.9, 133.5, 132.9, 129, 119. EIMS *m/z*: 216.

3b. m.p. 296–298 °C. ^{1}H-NMR (400 Hz DMSO-d_6, δ): 7.30 (d, 1H), 7.26 (d, 1H), 7.14–7.20 (t, 2H), 8.27 (s, 1H), 11.24 (s, 1H, NH), 11.40 (s, 1H, NH). EIMS *m/z*: 250.

3c. m.p. 252–254 °C. ^{1}H-NMR (400 Hz DMSO-d_6, δ): 7.50 (d, 2H), 8.01 (d, 2H), 8.20 (s, 1H), 11.20 (s, 1H, NH), 11.39 (s, 1H, NH). EIMS *m/z*: 250.

3d. m.p. 297–299 °C. ^{1}H-NMR (400 Hz DMSO-d_6, δ): 3.85 (s, 3H), 7.18 (d, 2H), 8.40 (d, 2H), 8.20 (s, 1H), 11.07 (s, 1H, NH), 11.19 (s, 1H, NH). EIMS *m/z*: 246.

3e. m.p. > 320 °C. ^{1}H-NMR (400 Hz DMSO-d_6, δ): 6.85–6.87 (d, 2H), 8.24 (s, 1H), 8.31–8.33 (d, 2H), 10.66 (s, 1H, OH) 11.12 (s, 1H, NH), 11.24 (s, 1H, NH). EIMS *m/z*: 232.

3f. m.p. 276 °C. ^{1}H-NMR (400 Hz DMSO-d_6, δ): 3.10 (s, 6H), 6.79 (d, 2H), 8.12 (s, 1H), 8.40 (d, 2H), 10.7 (s, 1H, NH), 11.05 (s, 1H, NH). EIMS *m/z*: 259.

3g. m.p. 266–268 °C. ^{1}H-NMR (400 Hz DMSO-d_6, δ): 6.52–6.82 (m, 2H), 7.82–7.10 (m, 5H), 8.20 (d, 1H), 11.29 (s, 1H, NH), 11.47 (s, 1H, NH). EIMS *m/z*: 242.

3h. m.p. 300–302 °C. ^{1}H-NMR (400 Hz DMSO-d_6, δ): 6.75 (d, 1H), 8.01 (s, 1H), 8.11 (s, 1H), 8.52 (d, 1H), 11.23 (s, 1H, NH), 11.31 (s, 1H, NH). EIMS *m/z*: 206.

3i. m.p. 290–292 °C. ^{1}H-NMR (400 Hz DMSO-d_6, δ): 2.50 (d, 3H), 6.46 (d, 1H), 8.04 (s, 1H), 8.51 (d, 1H), 11.12 (s, 1H, NH), 11.20 (s, 1H, NH). EIMS *m/z*: 221.

3j. m.p. 238–241 °C. ^{1}H-NMR (400 Hz DMSO-d_6, δ): 7.10 (t, 2H), 8.30 (s, 1H), 8.50 (dd, 1H), 8.11 (s, 1H), 11.32 (s, 1H, NH), 11.44 (s, 1H, NH). EIMS *m/z*: 261.

3k. m.p. > 300 °C. ^{1}H-NMR (400 Hz DMSO-d_6, δ): 3.76 (s, 3H), 3.85 (s, 3H), 7.3 (d, 1H), 7.86 (dd, 1H), 8.20 (s, 1H), 8.35 (d, 1H), 11.02 (s, 1H, NH), 11.04 (s, 1H, NH). EIMS *m/z*: 276.

3l. m.p. 162–164 °C. ^{1}H-NMR (400 Hz DMSO-d_6, δ): 6.67 (s, 1H), 2.05 (s, 3H), 7.92–7.04 (m, 5H), 8.09 (s, 1H), 11.27 (s, 1H, NH), 11.44 (s, 1H, NH). EIMS *m/z*: 256.

3m. m.p. > 320 °C. EIMS *m/z*: 255.

3n. m.p. 315–318 °C. ^{1}H-NMR (400 Hz DMSO-d$_6$, δ): 3.84 (s, 6H), 7.9 (s, 1H), 8.04 (s, 1H), 8.52 (s, 1H), 9.7 (s, 1H), 11.08 (s, 1H, NH), 11.21 (s, 1H, NH). EIMS *m/z*: 366.

3. Results and discussion

3.1. Characterization results of $CoFe_2O_4$ nanoparticles

The FT-IR spectra of $CoFe_2O_4$ showed peaks at 586.25, 1054.30, 1339.70, 1488.35, 1626.07, and 3370.93 cm^{-1} (Fig. 1). The peak observed at 586.25 cm^{-1} corresponds to the M–O tetrahedral site of the spinel structure, and this peak shows the basic nature of the nanoparticles obtained [47].

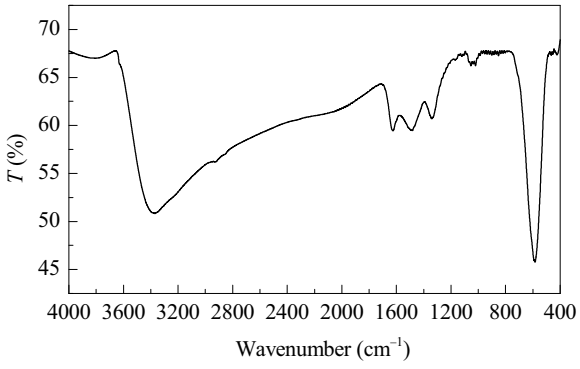

Fig. 1. FT-IR spectrum of $CoFe_2O_4$ nanoparticles.

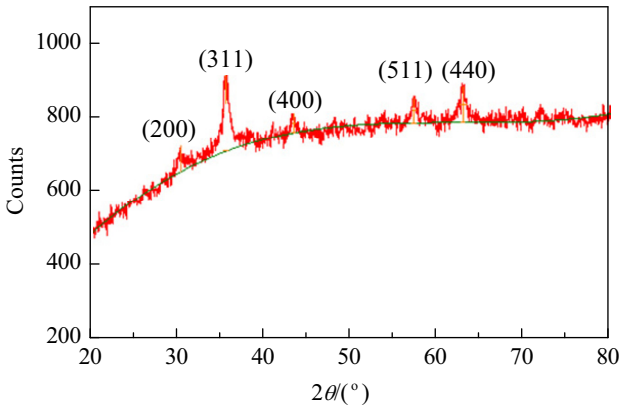

Fig. 2. XRD pattern of $CoFe_2O_4$ nanoparticles.

The XRD pattern of the $CoFe_2O_4$ nanoparticles is shown in Fig. 2. All the diffraction peaks and relative intensity match the JCPDS (International Center for Diffraction Data) PDF cards 3-864 and 22-1086 very well [48,49]. This revealed that the $CoFe_2O_4$ nanoparticles have cubic structure. The peak broadening indicates the nanocrystalline nature of the sample. The nanoparticle crystallite size was also determined from the XRD pattern using the Debye-Scherrer formula [50] and was found to be 2.87 nm, which is consistent with the particle size obtained from TEM analysis.

The structural composition was examined by EDX, as shown in Fig. 3. The EDX analysis showed the elemental distribution of $CoFe_2O_4$ and the presence of Co and Fe. The surface morphology was determined using SEM analysis, and the analysis showed that the nanoparticles had rough rocky surfaces, as shown in Fig. 4.

TEM was also used to determine the size and shape of the nanoparticles, and the TEM images are shown in Fig. 5. The average nanoparticle size was found to be in the range 2–8 nm, which is in agreement with the average size obtained from the XRD pattern. The TEM images showed that the nanoparticles were spherical.

Field-dependent magnetic measurements were performed on the $CoFe_2O_4$ nanoparticles at room temperature, using a

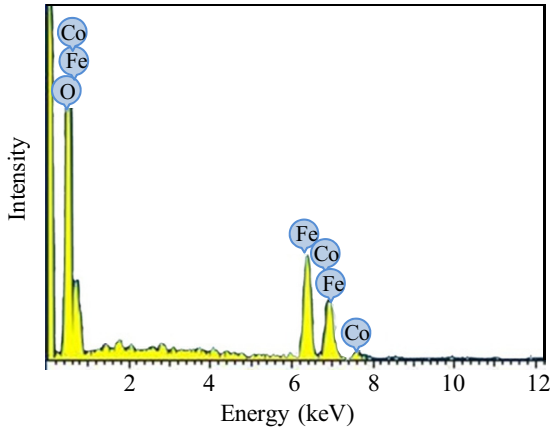

Fig. 3. EDX analysis of $CoFe_2O_4$ nanoparticles.

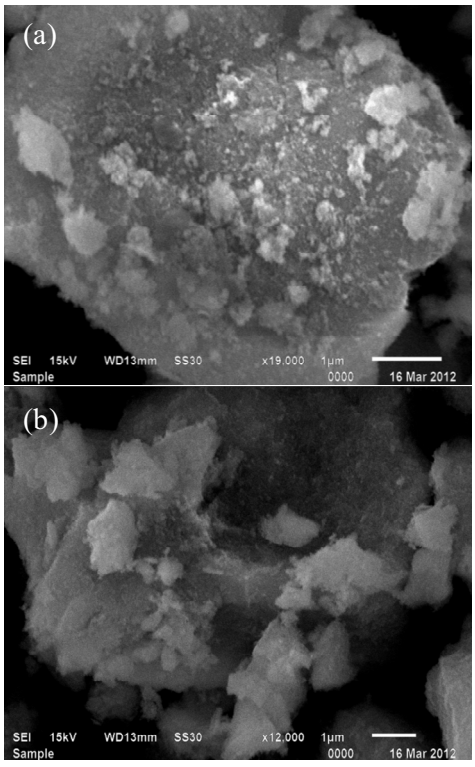

Fig. 4. SEM images of $CoFe_2O_4$ nanoparticles.

VSM, in the range from +1 T to −1 T, as shown in Fig. 6. The saturation magnetization (M_s), remanence (M_r), and coercivity (H_c) values were obtained from the hysteresis loop. The M_s was 1.77 emu/g, compared with the corresponding bulk value of 83 emu/g [51]. The H_c was 527 Oe; M_r was found to be 0.259 emu/g and the squareness ratio (M_r/M_s) was 0.146. The decrease in M_s compared with that of the bulk material is primarily caused by the effect of the small particle surface area, which

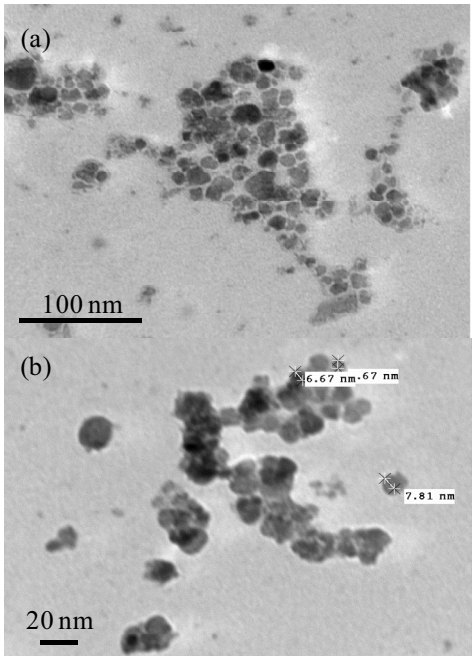

Fig. 5. TEM images of $CoFe_2O_4$ nanoparticles.

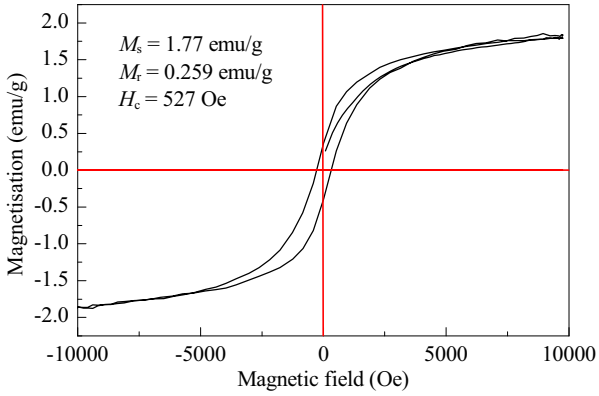

Fig. 6. Field-dependent magnetization of $CoFe_2O_4$ nanoparticles.

becomes prominent as the particle size decreases [52]. The curve shows almost no hysteresis and is reversible. The size of the $CoFe_2O_4$ nanoparticles is below the superparamagnetic critical size, as confirmed by TEM (2–8 nm). The synthesized nanoparticles therefore show superparamagnetic characteristics.

The surface area is an important parameter for catalysis. The surface area of the $CoFe_2O_4$ nanoparticles was determined using the BET equation [53], and was found to be 140.9 m^2/g, calculated from the BET plot in Fig. 7; this is much higher than the surface area of bulk cobalt ferrite [54–56]. The higher surface area is an advantage in improving catalytic performance.

Finally, the stability of the $CoFe_2O_4$ nanoparticles was determined using TGA; the results are shown in Fig. 8. The TGA pattern shows that an initial mass loss occurred up to 150 °C as a result of evaporation of adsorbed water and the presence of volatile components. The further mass loss observed between 150 °C and 360 °C may be caused by loss of structural water or hydroxyl groups on the sample surface. The final decomposition temperature was at around 361 °C; no further mass loss was detected up to 700 °C, which showed the thermal stability of the catalyst. Two peaks, one endothermic and the other exothermic, were observed in the corresponding DTA pattern. The rate of decomposition per minute at the corresponding TGA temperature was also determined, and this showed that at 352.3 °C the rate of decomposition was only 179 μg/min, which further supports the thermal stability of the catalyst.

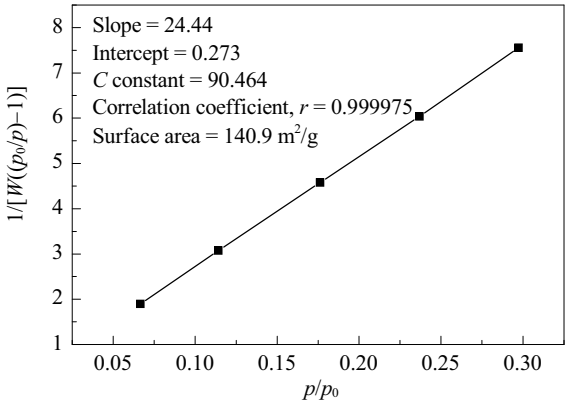

Fig. 7. BET plot of $CoFe_2O_4$ nanoparticles.

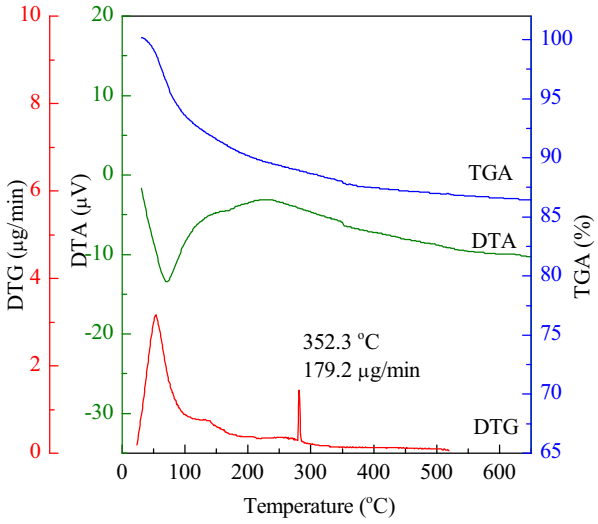

Fig. 8. TGA/DTA/DTG analysis of $CoFe_2O_4$ nanoparticles.

3.2. *Catalytic application of $CoFe_2O_4$ nanoparticles in synthesis of arylidene barbituric acid derivatives*

To investigate the catalytic activity of the synthesized catalyst, the $CoFe_2O_4$ nanoparticles were used in the synthesis of arylidene barbituric acid derivatives.

To study the efficiency of the $CoFe_2O_4$ nanocatalyst, benzaldehyde (**1a**) and barbituric acid (**1b**) were used as the model substrate (Table 1). The product **3a** was obtained in 40% yield in CH_3CN at room temperature with $CoFe_2O_4$ (5 mol%) as the catalyst (Table 1, entry 1). The yield of **3a** increased to 94% using a water-ethanol (1:1) mixture (Table 1, entry 9), but other solvents did not give better results (Table 1, entries 1–8). This is because the solvent affects the transition state, and when polar substrates are used in the synthesis, the transition state is better solvated and the reaction rate increases, which increases the product yield [57,58]. In optimizing the reaction conditions, the amount of catalyst was the major factor. The model reaction was studied using 2, 5, 10, 15, and 20 mol% of

Table 1
Optimization of reaction conditions using $CoFe_2O_4$ nanocatalyst.

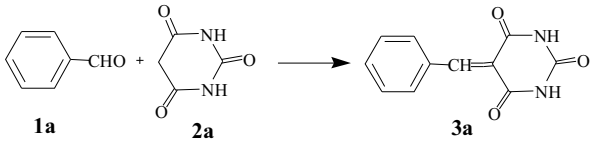

1a **2a** **3a**

Entry	Catalyst amount (mol%)	Solvent	Isolated yield (%)
1	5	CH_3CN	40
2	5	EtOAc	48
3	5	DCM	50
4	5	H_2O	67
5	5	EtOH	79
6	5	H_2O: EtOH (1:3)	85
7	5	H_2O: EtOH (1:2)	89
8	2	H_2O: EtOH (1:1)	85
9	5	H_2O: EtOH (1:1)	94
10	10	H_2O: EtOH (1:1)	95
11	15	H_2O: EtOH (1:1)	94
12	20	H_2O: EtOH (1:1)	92
13	5 [a]	H_2O: EtOH (1:1)	70
14	—	H_2O: EtOH (1:1)	50

Reaction conditions: **1a** (5 mmol), **2a** (5 mmol), catalyst (5 mol%), solvent (5 ml), room temperature.
[a] Bulk $CoFe_2O_4$.

Table 2
Synthesis of derivatives of arylidene barbituric acid, **3a**–**3n**, in the presence of $CoFe_2O_4$ nanocatalyst.

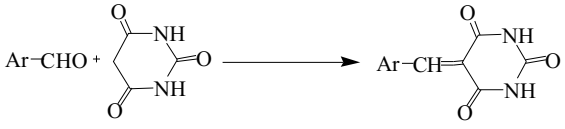

1a–**1n** **2** **3a**–**3n**

Entry	Ar	Product	Time (min)	Isolated yield (%)	TOF [a] (h^{-1})	m.p.	
						Observed	Reported
1	C_6H_5	**3a**	4	94	1666.7	262–264	263–265
2	4-Cl C_6H_4	**3b**	2	91	3333.3	296–298	298.5
3	2-Cl C_6H_4	**3c**	5	89	1250	252–254	254
4	4-$OCH_3C_6H_4$	**3d**	4	88	1666.7	297–299	298–300
5	4-OH C_6H_4	**3e**	5	86	1250	>320	—
6	4-$(CH_3)_2N$ C_6H_4	**3f**	3	90	2000	276	274–276
7	C_6H_5CH=CH	**3g**	2	87	3333.3	266–268	270
8	Furyl	**3h**	5	85	1250	300–302	257–259
9	5-Me-Furyl	**3i**	6	86	1000	290–292	—
10	3-NO_2 C_6H_4	**3j**	3	80	2000	238–241	248–250
11	3,4-$(OCH_3)_2$ C_6H_3	**3k**	3	87	2000	>300	>290
12	α- Me-C_6H_4CH=CH	**3l**	2	82	1666.7	162–164	228–229
13	Indole-3-carboxyaldehyde	**3m**	5	82	1250	>320	—
14	Syringaldehyde	**3n**	4	88	1666.7	315–318	—

Reaction conditions: aldehyde (5 mmol), barbituric acid (5 mmol), $CoFe_2O_4$ (5 mol%), water-ethanol (1:1) 5 ml, room temperature.
[a] Turnover frequency (moles of reactant converted/(moles of catalyst × reaction time)).

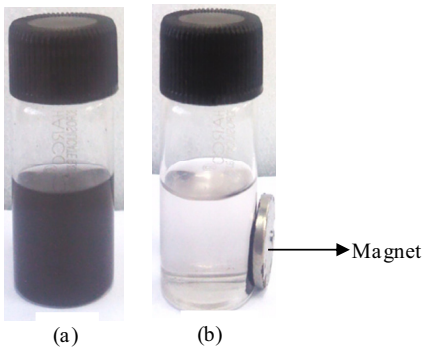

Fig. 9. Dispersion of $CoFe_2O_4$ nanoparticles in water-ethanol 1:1 mixture (a) and magnetic separation of catalyst (b).

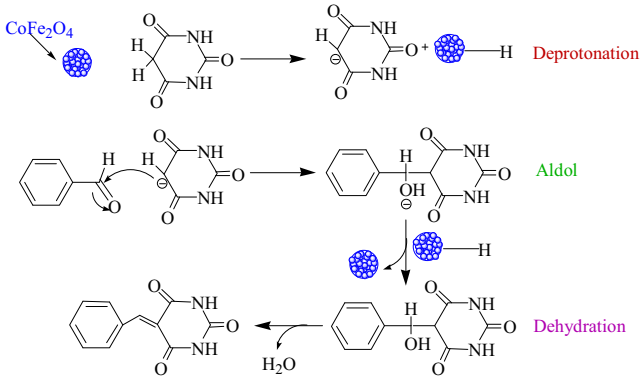

Scheme 1. Proposed mechanism for synthesis of arylidene barbituric acid **3a** using $CoFe_2O_4$ nanocatalyst.

catalyst. Of these, 5 mol% of catalyst was found to be the optimum amount for the reaction (Table 1, entry 9); when the catalyst loading was less than 5 mol%, the yield decreased significantly (Table 1, entry 8), but increasing the catalyst loading above 5 mol% did not improve the yield (Table 1, entries 10–12).

In the absence of the catalyst, only a trace amount of the product was obtained (Table 1, Entry 14). The reaction was carried out using bulk $CoFe_2O_4$ but the yield was only 70% (Table 1, entry 13), compared with 94% using the nanocatalyst (Table 1, entry 9).

Under the optimized reaction conditions, a series of aldehydes was investigated to establish the scope and limitations of this synthesis (Table 2). The reaction was extended using various aldehydes, namely heteroatom aldehydes (Table 2, entries 8, 9 and 13), unsaturated aldehydes (Table 2, entries 7 and 12), and aldehydes with electron-withdrawing or electron-donating substituents at the *ortho*-, *meta*-, and *para*- positions; all these aldehydes gave the desired products in good to excellent yields (Table 2, entries 2–14). The reactions were clean, and completion of the reaction was monitored by formation of a colored product. After the reaction was complete, the catalyst was separated out from the reaction mixture using an external magnet (Fig. 9). The products were purified by recrystallization and characterized using FT-IR and ^{1}H-NMR spectroscopies. The products were formed with good chemoselectivity and no side-product formation was observed during the synthesis. The synthetic protocol has good turnover frequencies (1000–1666.7 h^{-1}) (Table 2). The Lewis basic sites in the cobalt ferrite nanoparticles are responsible for the present organic transformation. The Lewis basic sites originate from electrons trapped in intrinsic defects, from surface hydroxyl groups [59], or from coordinatively unsaturated oxide ions associated with neighboring hydroxyl groups [60]. A proposed mechanism for the reaction is given in Scheme 1.

Arylidene barbituric acid derivatives have previously been synthesized using various methods, but these methods either gave low yields or involved complex reaction conditions (Table 3). The present method is efficient and the catalyst used is an excellent catalyst.

3.3. *Recovery and reusability of catalyst*

One advantage of $CoFe_2O_4$ nanoparticles is their ability to act as heterogeneous recyclable reaction systems. After completion of the reaction between benzaldehyde and barbituric acid, the catalyst was separated quantitatively (> 97%) from the reaction mixture using a magnetic separator and then

Table 3
Synthesis of arylidene barbituric acid derivatives in presence of different catalysts.

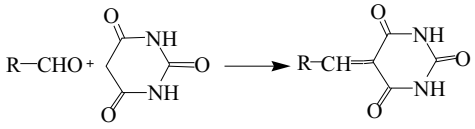

No.	Substrate (R-CHO)	Catalyst	Reaction condition	Yield (%)	Ref.
1	C_6H_5CHO	$Ce_1Mg_xZr_{1-x}O_2$	Solvent free, MW, 450 W/3 min	90	[39]
2	C_6H_5CHO	PVP Ni Nanoparticles	Ethylene glycol, 50 °C/10–15 min	91	[36]
3	C_6H_5CHO	Basic alumina	Solvent free, MW, 700 W/5 min	90	[32]
4	C_6H_5CHO	$SiO_2{\cdot}12WO_3{\cdot}24H_2O$	Water, ultrasound/10 min	61	[41]
5	3- $NO_2C_6H_4CHO$	NH_2SO_3H	Grinding/10 min	47	[35]
6	C_6H_5CHO	NH_4-OAc/AcOH	MW, 560 W/7 min	52	[35]
7	Indole-3-carboxyaldehyde	L-proline	Ethanol, 60 °C/3.5 h	60	[37]
8	4- ClC_6H_4CHO	$BiCl_3$	R.T./30 min	85	[38]
9	4- ClC_6H_4CHO	TEBA	Water, 70 °C/2 h	84	[42]
10	C_6H_5CHO	KSF clay	MW, 560 W/7 min	70	[33]
11	C_6H_5CHO	NaCl	MW, 560 W/7 min	68	[33]
12	C_6H_5CHO	$CoFe_2O_4$ nanoparticles	Aq. ethanol/R.T./4 min	94	this work

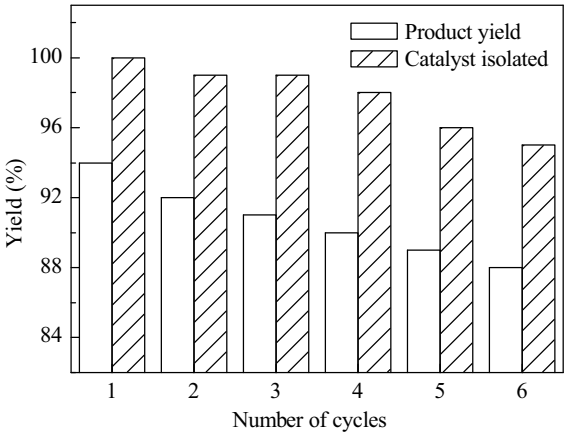

Fig. 10. The recyclability of $CoFe_2O_4$ nanoparticles for synthesis of **3a**.

washed with ethanol, followed by drying at 70 °C for 1 h. The nanoparticles were reused six times for the synthesis of arylidene barbituric acid derivatives without significant loss of activity. The catalytic performance of $CoFe_2O_4$ was found to be unaltered (up to six consecutive cycles). This method is potentially an important protocol for large-scale synthesis. The recycling results are shown in Fig. 10.

4. Conclusions

The present protocol highlights the use of $CoFe_2O_4$ nanoparticles as a green, inexpensive, efficient, simple, non-toxic, and recoverable catalyst for the synthesis of arylidene barbituric acid derivatives. The synthesized spinel-shaped $CoFe_2O_4$ nanoparticles have advantageous properties such as a small particle size (2–8 nm), high surface area, and a magnetic nature, which make them an excellent catalyst for the present synthetic protocol. The attractive features of this synthesis are a short reaction time, high turnover frequency, simple work-up process, a clean reaction, non-toxic reagents, an aqueous medium, recovery/recyclability of the catalyst, ecofriendly synthesis, and excellent yields of products, making it an excellent alternative to other reported protocols.

Acknowledgments

We are thankful to SAIF, Panjab University Chandigarh for FT-IR, TEM, ^{1}H-NMR, and ^{13}C-NMR, IIT Ropar for SEM and XRD, CIL IIT Roorkee for VSM, and NML Jamshedpur for BET. One of the authors (G.K.) is thankful to MHRD and NIT Jalandhar for providing the research fellowship.

References

[1] Anastas P T, Warner J C. Green Chemistry: Theory and Practice. Oxford: Oxford University, 1998
[2] Guin D, Baruwati B, Manorama S V. *Org Lett*, 2007, 9: 1419
[3] Sun S H, Zeng H. *J Am Chem Soc*, 2002, 124: 8204
[4] Latham A H, Williams M E. *Acc Chem Res*, 2008, 41: 411
[5] Laurent S, Forge D, Port M, Roch A, Robic C, Elst L V, Muller R N. *Chem Rev*, 2008, 108: 2064
[6] Kawamura M, Sato K. *Chem Commun*, 2006: 4718
[7] Phan N T S, Gill C S, Nguyen J V, Zhang Z J, Jones C W. *Angew Chem Int Ed*, 2006, 45: 2209
[8] Aschwanden L, Panella B, Rossbach P, Keller B, Baiker A. *ChemCatChem*, 2009, 1: 111
[9] Zhang Y, Xia C G. *Appl Catal A*, 2009, 366: 141
[10] Gill C S, Long W, Jones C W. *Catal Lett*, 2009, 131: 425
[11] Li J, Zhang Y M, Han D F, Gao Q, Li C. *J Mol Catal A*, 2009, 298: 31
[12] Schötz A, Hager M, Reiser O. *Adv Funct Mater*, 2009, 19: 2109
[13] Polshettiwar V, Varma R S. *Tetrahedron*, 2010, 66: 1091
[14] Ranganath K V S, Kloesges J, Schäfer A H, Glorius F. *Angew Chem Int Ed*, 2010, 49: 7786
[15] Sato Turtelli R, Duong G V, Nunes W, Groessinger R, Knobel M. *J Magn Magn Mater*, 2008, 320: e339
[16] Murdock E S, Simmons R F, Davidson R. *IEEE Trans Magn*, 1992, 28: 3078
[17] Shafi K V P M, Gedanken A, Prozorov R, Balogh J. *Chem Mater*, 1998, 10: 3445
[18] Liu C, Rondinone A J, Zhang Z J. *Pure Appl Chem*, 2000, 72: 37
[19] Yang H M, Zhang X C, Tang A D, Oiu G Z. *Chem Lett*, 2004, 33: 826
[20] Olsson R T, Salazar-Alvarez G, Hedenqvist M S, Gedde U W, Lindberg F, Savage S J. *Chem Mater*, 2005, 17: 5109
[21] Bhattacharyya S, Salvetat J P, Fleurier R, Husmann A, Cacciaguerra T, Saboungi M L. *Chem Commun*, 2005: 4818
[22] Sun S H, Zeng H, Robinson D B, Raoux S, Rice P M, Wang S X, Li G X. *J Am Chem Soc*, 2004, 126: 273
[23] Anil Kumar P S, Shrotri J J, Kulkarni S D, Deshpande C E, Date S K. *Mater Lett*, 1996, 27: 293
[24] Akopyan L G, Adzhibekyan A S, Darbinyan G A, Tumasyan E A. *Biol Zh Arm*, 1976, 29: 80; *Chem Abstr*, 1976, 85: 72068f
[25] Chaaban I, Mohsen A, Omar M E, Maharan M A. *Sci Pharm*, 1984: 52; *Chem Abstr*, 1984, 101: 75677a
[26] Jursic B S. *J Heterocycl Chem*, 2001, 38: 655
[27] Frangin Y, Guimbal C, Wissocq F, Zamarlik H. *Synthesis*, 1986, 12: 1046
[28] Bojarski J T, Mokrosz J L, Barton H J, Paluchowska M H. *Adv Heterocycl Chem*, 1985, 38: 229
[29] Figueroa-Villar J D, Cruz E R, Lucia dos Santos N. *Synth Commun*, 1992, 22: 1159
[30] Ikeda H, Kawabe Y, Sakai T, Kawasaki K. *Chem Lett*, 1989, 18: 1803
[31] Rezende M C, Campodonico P, Abuin E, Kossanyi J. *Spectrochim Acta Part A*, 2001, 57: 1183
[32] Khalafi-Nezhad A, Hashemi A. *Iran J Chem Chem Eng*, 2001, 20: 9
[33] Alcerreca G, Sanabria R, Miranda R, Arroyo G, Tamariz J, Delgado F. *Synth Commun*, 2000, 30: 1295
[34] Dewan S K, Singh R. *Synth Commun*, 2003, 33: 3081
[35] Li J T, Dai H G, Liu D, Li T S. *Synth Commun*, 2006, 36: 789
[36] Khurana J M, Vij K. *Catal Lett*, 2010, 138: 104
[37] Jain S, Bhimireddy N R, Kolisetty S R. *Int J ChemTech Res*, 2011, 3: 817
[38] Khan K M, Ali M, Farooqui T A, Khan M, Taha, M, Perveen S. *J Chem Soc Pak*, 2009, 31: 823
[39] Rathod S B, Gambhire A B, Arbad B R, Lande M K. *Bull Korean Chem Soc*, 2010, 31: 339
[40] Wang C, Ma J J, Zhou X, Zang X H, Wang Z, Gao Y J, Cui P L. *Synth Commun*, 2005, 35: 2759
[41] Li J T, Sun M X. *Aust J Chem*, 2009, 62: 353
[42] Shi D Q, Chen J, Zhung Q Y, Wang X S, Hu H W. *Chin Chem Lett*, 2003, 14: 1242
[43] Rajput J K, Kaur G. *Tetrahedron Lett*, 2012, 53: 646
[44] Sharma D, Rajput J, Kaith B S, Kaur M, Sharma S. *Thin Solid Films*,

Graphical Abstract

Chin. J. Catal., 2013, 34: 1697–1704 doi: 10.1016/S1872-2067(12)60646-9

$CoFe_2O_4$ nanoparticles: An efficient heterogeneous magnetically separable catalyst for "click" synthesis of arylidene barbituric acid derivatives at room temperature

Jaspreet Kaur Rajput*, Gagandeep Kaur
Dr. B. R. Ambedkar National Institute of Technology, Jalandhar, India

An efficient protocol for the "click" synthesis of arylidene barbituric acid derivatives using a heterogeneous magnetically separable $CoFe_2O_4$ nanocatalyst is presented. The synthesis is simple, clean, and eco-friendly.

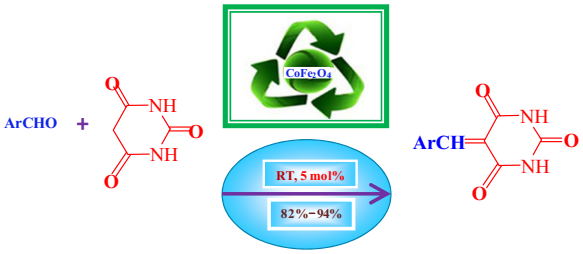

2010, 519: 1224
[45] Sharma D, Sharma S, Kaith B S, Rajput J, Kaur M. *Appl Surf Sci*, 2011, 257: 9661
[46] Borgohain C, Senapati K K, Mishra D, Sarma K C, Phukan P. *Nanoscale*, 2010, 2: 2250
[47] Ramankutty C G, Sugunan S. *Appl Catal A*, 2001, 218: 39
[48] Cao X B, Li G. *Nanotechnology*, 2005, 16: 180
[49] Hyeon T, Chung Y, Park J, Lee S S, Kim Y W, Park B H. *J Phys Chem B*, 2002, 106: 6831
[50] Cullity B D. Elements of X-Ray Diffraction. London: Addision Wesely, 1959. 261
[51] Rashad M M, Mohamed R M, Ibrahim M A, Ismail L F M, Abdel-Aal E A. *Adv Powder Technol*, 2012, 23: 315
[52] Martinez B, Obradors X, Balcells L, Rouanet A, Monty C. *Phys Rev Lett*, 1998, 80: 181
[53] Greg S J, Sing K S W. Adsorption, Surface Area, and Porosity. New York: Academic, 1982
[54] Senapati K K, Borgohain C, Phukan P. *J Mol Catal A*, 2011, 339: 24
[55] Jiao Z, Geng X, Wu M H, Jiang Y, Zhao B. *J Colloid Surf A*, 2008, 313-314: 31
[56] Senapati K K, Roy S, Borgohain C, Phukan P. *J Mol Catal A*, 2012, 352: 128
[57] Gascon J, Aktay U, Hernandez-Alonso M D, van Klink G P M, Kapteijn F. *J Catal*, 2009, 261: 75
[58] Corma A, Iborra S, Rodriguez I, Sanchez F. *J Catal*, 2002, 211: 208
[59] Meguro K, Esumi K. *J Adhesion Sci Technol*, 1990, 4: 393
[60] Cordischi D, Indovina V. *J Chem Soc, Faraday Trans I*, 1976, 72: 2341